Adiabatic theorem and continuous coupled-mode theory for efficient taper transitions in photonic crystals

Steven G. Johnson,[1,*] Peter Bienstman,[1] M. A. Skorobogatiy,[2] Mihai Ibanescu,[1] Elefterios Lidorikis,[1] and J. D. Joannopoulos[1]
[1]*Department of Physics, Massachusetts Institute of Technology, Cambridge, Massachusetts 02139*
[2]*OmniGuide Communications, One Kendall Square, Cambridge, Massachusetts 02139*
(Received 28 June 2002; published 18 December 2002)

We prove that an adiabatic theorem generally holds for slow tapers in photonic crystals and other strongly grated waveguides with arbitrary index modulation, exactly as in conventional waveguides. This provides a guaranteed pathway to efficient and broad-bandwidth couplers with, e.g., uniform waveguides. We show that adiabatic transmission can only occur, however, if the operating mode is propagating (nonevanescent) and guided at every point in the taper. Moreover, we demonstrate how straightforward taper designs in photonic crystals can violate these conditions, but that adiabaticity is restored by simple design principles involving only the independent band structures of the intermediate gratings. For these and other analyses, we develop a generalization of the standard coupled-mode theory to handle arbitrary nonuniform gratings via an instantaneous Bloch-mode basis, yielding a continuous set of differential equations for the basis coefficients. We show how one can thereby compute semianalytical reflection and transmission through crystal tapers of almost any length, using only a single pair of modes in the unit cells of uniform gratings. Unlike other numerical methods, our technique becomes *more* accurate as the taper becomes more gradual, with no significant increase in the computation time or memory. We also include numerical examples comparing to a well-established scattering-matrix method in two dimensions.

DOI: 10.1103/PhysRevE.66.066608 PACS number(s): 42.70.Qs, 42.79.Dj, 42.82.Et

I. INTRODUCTION

Waveguides with strong ''gratings,'' i.e., large axial index modulation, are increasingly important components of optical devices, from filters to distributed-feedback lasers—they especially arise in the context of photonic crystals, periodic dielectric structures with a band gap that forbids propagation of light for a range of frequencies along some (possibly all) directions [1]. Such waveguides can exhibit high transmission around sharp bends [2] or through wide-angle splitters [3], form a robust substrate for interacting with resonators and filters [4], may have dramatically slow group velocities and anomalous dispersion, and can greatly amplify nonlinear phenomena [5,6]. In all such applications, however, one question that arises is how to couple them efficiently with conventional (nongrated) waveguides; this is especially challenging for slow-light waveguides (near band edges or from coupled resonators [7]) due to their large ''impedance'' mismatch. In this paper, we prove that, as for conventional waveguides [8], an *adiabatic theorem* ensures that sufficiently slow transitions (tapered, or ''apodized,'' gratings) produce arbitrarily good transmission between grated and nongrated waveguides. Although the general concept of slow transitions in grated waveguides has been previously implemented on a trial-and-error basis [9–14], the existence of the adiabatic limit was unproven. We find that this theorem, moreover, imposes two requirements on the taper that lead directly to design principles.

(i) The operating mode must *not be evanescent* (cannot lie in a band gap) for any intermediate point of the taper.

(ii) The operating mode must *be guided* (i.e., not part of a continuum) for every intermediate point of the taper. (Or, if leaky, the leakage rate should be slow compared to the taper.)

In fact, both of these common-sense criteria hold for tapers of nongrated waveguides as well: no one would expect high transmission if a conventional waveguide were tapered to be narrower than the cutoff for guiding and then tapered back. The conditions take on a new importance, however, for photonic crystals and strong gratings, because here the most ''obvious'' taper designs can inadvertently violate them. We demonstrate how this occurs in an example two-dimensional system, and how adiabaticity can be restored by simple modifications (varying the period and/or ''unzipping'' the crystal) based on an inexpensive band-structure analysis of uniform gratings at intermediate points in the taper.

Furthermore, in order to prove the adiabatic theorem, we develop a generalization of coupled-mode theory [8,15] to arbitrary grated waveguides, yielding a continuous set of ordinary differential equations for the coefficients of ''instantaneous'' Bloch modes at each point in a taper. These equations enable the semianalytical computation of reflection and transmission through grating tapers not limited in index contrast or geometry. We thereby demonstrate how accurate results are obtained by combining independent calculations for the unit cells of intermediate points in a taper, with the basis so efficient that typically only a single pair of eigenstates are required. Unlike other numerical techniques such as finite-difference time-domain methods [16] or transfer/scattering matrices [17–21], these coupled-mode equations can yield the transmission for many taper rates simultaneously with essentially no additional computational effort. In fact, our method becomes *more* accurate (and no more expensive) as the taper becomes more gradual, rather than requiring ever-

*Electronic address: stevenj@alum.mit.edu

increasing spatial resolution and computational power.

Coupled-mode theory generally involves expanding the electromagnetic fields in some basis, typically the eigenmodes of a waveguide, and then solving for the basis coefficients as a function of position. There exist many variations on this theme, but they can broadly be divided according to the expansion basis and the method of solving for the coefficients. (We do not consider coupled-mode theories for coupling *parallel* waveguides, which have a special set of concerns such as nonorthogonality [22].) The classic expansion basis at each point is that of the ''instantaneous'' eigenmodes (or quasimodes) of an infinite straight/uniform waveguide matching the cross section at that point. If the cross section is a continuously varying quantity, this yields a set of coupled differential equations for the mode coefficients, where the coupling is due only to the rate of *change* of the cross section [8,15]—thus, they efficiently express the low scattering that occurs in slowly changing structures. In the presence of a grating, these equations are most commonly solved using only the fundamental Fourier component of the index modulation, which is valid only in the limit of weak gratings [8,23–25], but a more complete basis can also be employed at a greater computational expense. (In one dimension, an exact theory can be formulated by forcing an equivalence to the analytical transfer matrices [26].) Alternatively, if the cross section is piecewise-constant, one obtains a scattering-matrix or transfer-matrix method as referenced above, also called rigorous coupled-wave analysis, mode matching, and so on; there, the mode coefficients change discontinuously at a discrete set of points where the boundary conditions are matched. All such instantaneous eigenmode techniques, however, suffer in efficiency when faced with a strong grating: the mode coefficients change rapidly with the cross section, so a large basis is required even for a periodic grating where, in principle, there is no scattering. A more natural basis for strong gratings is that of the Bloch modes [1], which have constant coefficients for a periodic grating and should therefore be an efficient representation in gratings with slow (or rare) change. Such a basis has been employed for scattering-matrix formulations, in which the Bloch modes of a *discrete* set of locally uniform gratings are matched at their boundaries [11,19]. Although this is an effective computational tool, it still involves a discontinuous change of the basis coefficients and so it is suboptimal for slow tapers compared to the *continuously* changing grating representation that we develop here. Our method is the natural analog of the classical treatment of ordinary tapers in terms of instantaneous eigenmodes. Moreover, the continuous representation especially lends itself to analytic study (even beyond the adiabatic theorem itself). For example, we immediately find that the scattered/reflected power falls with the square of the taper length, and oscillates at a rate given by the phase-velocity mismatch with the scattered mode. A related problem has been studied in a continuous Bloch basis for quantum mechanics, that of a slowly modulated time-oscillatory Hamiltonian—there, the analysis is greatly complicated by the fact that the eigenvalue spectrum is unbounded and becomes dense in the presence of the oscillation [27,28]. Finally, we should mention that another possible basis is that of the eigenmodes of a *fixed* waveguide or grating [15], which is useful to handle small deviations from an ideal waveguide, but not for transitions between greatly differing waveguides. The Bloch modes of a grating can then be straightforwardly employed, and this has been used to study, e.g., nonlinear perturbations in periodic waveguides [29].

In the following, we begin by introducing a Hermitian eigenproblem formulation of the fully vectorial Maxwell's equations for propagation of definite-frequency states, providing an abstract algebraic framework that greatly simplifies the problem, and we point out some important differences compared to, e.g., quantum mechanics. Second, we review the derivation of standard coupled-mode theory for nongrated waveguides in this framework. Section IV then generalizes this treatment to arbitrary grated waveguides, eventually arriving at coupled-mode equations that are of almost exactly the same form as the familar result—thus, the adiabatic theorem immediately follows (the proof is identical). Also discussed are important considerations in practical computations with these coupled-mode equations. Finally, in Sec. V we illustrate the theory by comparing it to an ''exact'' scattering-matrix method in two dimensions, and in Sec. VI describe pitfalls and simple design criteria for constructing adiabatic transitions. There are also two appendixes, one outlining a proof of the adiabatic theorem and highlighting the origin of the conditions it imposes, and the other discussing important phase choices that arise in the Bloch basis (in analog to Berry's phase [30,31] from quantum mechanics).

II. WAVEGUIDES AND DIRAC NOTATION

In this paper, we employ the Dirac notation of abstract linear operators $\hat{A}$ and state kets $|\psi\rangle$ [32,33] to cast Maxwell's equations at a fixed frequency ω as a Hermitian eigensystem in explicit analogy with quantum mechanics (with the spatial propagation direction z taking the place of t). Here, the analogs to the quantum-mechanical potential are the dielectric function $\varepsilon(x,y,z)$ and the magnetic permeability $\mu(x,y,z)$. Unlike most previous work with photonic crystals, where one finds ω eigenvalues at a fixed wave vector [1], we will find *wave vector* eigenvalues at a fixed ω: only frequency is conserved in a nonuniform waveguide, and we are interested in the field profile as a function of z.

By moving all of the z derivatives to one side and expressing $\{E_z, H_z\}$ in terms of the transverse fields $\{\mathbf{E}_t, \mathbf{H}_t\}$, the fully vectorial source-free Maxwell's equations for time-harmonic states are easily rewritten in the form [34,35]

$$\hat{A}|\psi\rangle = -i\frac{\partial}{\partial z}\hat{B}|\psi\rangle, \tag{1}$$

where $|\psi\rangle$ is the four-component column vector,

$$|\psi\rangle \equiv \begin{pmatrix} \mathbf{E}_t(x,y,z) \\ \mathbf{H}_t(x,y,z) \end{pmatrix} e^{-i\omega t}, \tag{2}$$

and $\hat{A}$ and $\hat{B}$ are

$$\hat{A} \equiv \begin{pmatrix} \omega\varepsilon/c - \frac{c}{\omega}\boldsymbol{\nabla}_t \times \frac{1}{\mu}\boldsymbol{\nabla}_t \times & 0 \\ 0 & \omega\mu/c - \frac{c}{\omega}\boldsymbol{\nabla}_t \times \frac{1}{\varepsilon}\boldsymbol{\nabla}_t \times \end{pmatrix}, \tag{3}$$

$$\hat{B} \equiv \begin{pmatrix} 0 & -\hat{\mathbf{z}}\times \\ \hat{\mathbf{z}}\times & 0 \end{pmatrix} = \begin{pmatrix} & & & -1 \\ & & -1 & \\ & 1 & & \\ 1 & & & \end{pmatrix} = \hat{B}^{-1}, \tag{4}$$

where $\boldsymbol{\nabla}_t$ denotes the transverse (xy) components of $\boldsymbol{\nabla}$. $\hat{A}$ and $\hat{B}$ are *Hermitian* operators (for real/lossless ε and μ) under the inner product of two states $|\psi\rangle$ and $|\psi'\rangle$ given by

$$\langle\psi|\psi'\rangle \equiv \int \mathbf{E}_t^* \cdot \mathbf{E}_t' + \mathbf{H}_t^* \cdot \mathbf{H}_t'. \tag{5}$$

Above, we have *not* made any approximations, paraxial or otherwise; Eq. (1) represents the full Maxwell's equations. In this way, we can analyze and exploit the linear algebraic structure of electromagnetism without wading through the usual three-dimensional mire of curls and components. Moreover, we show that many results such as orthonormality relations (as well as, e.g., perturbation theory [34–36]) follow automatically from well-known properties of Hermitian eigensystems, without requiring cumbersome rederivation in terms of explicit vector fields [8].

The constant matrix $\hat{B}$ couples the **E** and **H** fields and plays the role of a "metric" in, e.g., the orthonormality relations below, with Eq. (4) giving

$$\langle\psi|\hat{B}|\psi'\rangle = \hat{\mathbf{z}} \cdot \int \mathbf{E}_t^* \times \mathbf{H}_t' + \mathbf{E}_t' \times \mathbf{H}_t^*. \tag{6}$$

Thus, $\langle\psi|\hat{B}|\psi\rangle$ is simply $4P$, where P is the time-average power flowing in the $\hat{\mathbf{z}}$ direction. A key difference from quantum mechanics is that neither $\hat{A}$ nor $\hat{B}$ is positive definite, which has important implications for the eigenstates and orthonormality relations below.

Bloch waves, eigenstates, and orthonormality

For a waveguide with uniform cross section (z invariant ε and μ), the field $|\psi\rangle \equiv |\beta\rangle$ can be chosen to have z dependence $e^{i\beta z}$ [8], in which case Eq. (1) becomes the eigenproblem,

$$\hat{A}|\beta\rangle = \beta\hat{B}|\beta\rangle. \tag{7}$$

More generally, suppose that ε and μ are *periodic* functions of z with period ("pitch") Λ. In this case, the Bloch-Floquet theorem [1,37] tells us that the solutions can be chosen of the form of Bloch waves $e^{i\beta z}|\beta\rangle$, where $|\beta\rangle$ is now a *periodic* function with period Λ satisfying the Hermitian eigenproblem,

$$\hat{C}|\beta\rangle \equiv \left(\hat{A} + i\frac{\partial}{\partial z}\hat{B}\right)|\beta\rangle = \beta\hat{B}|\beta\rangle, \tag{8}$$

defining $\hat{C} \equiv \hat{A} + i(\partial/\partial z)\hat{B}$. Such solutions satisfy all the usual properties of Hermitian eigenproblems [32], e.g., orthogonality: $\langle\beta^*|\hat{B}|\beta'\rangle = 0$ as long as $\beta \neq \beta'$ ($|\beta^*\rangle$ is the eigenstate with conjugated eigenvalue β^*). Note the complex conjugation: because the eigenoperators are not positive definite, the eigenvalues β are only real when $\langle\beta|\hat{B}|\beta\rangle \neq 0$ (imaginary β corresponds to evanescent modes)—this is a significant departure from the real eigenvalues of quantum mechanics, and requires such an extended form of the orthogonality relation. For the case of a uniform waveguide ($\hat{C} = \hat{A}$) where the eigenoperators are real symmetric, we can choose $|\beta^*\rangle = |\beta\rangle^*$ and $\langle\beta^*|\hat{B}|\beta'\rangle$ becomes the well-known *unconjugated* $\mathbf{E}_t \times \mathbf{H}_t$ power-orthogonality relation that is usually derived from Lorentz reciprocity [8,15,54]. (Moreover, in uniform waveguides, this orthogonality holds even for complex ε, since $\hat{A}$ is then non-Hermitian but still complex symmetric.)

A corollary of Bloch's theorem tells us that the eigenmodes at β and $\beta + (2\pi/\Lambda)\ell$ are equivalent for any integer ℓ. In particular,

$$\left|\beta + \frac{2\pi}{\Lambda}\ell\right\rangle = e^{(-2\pi i/\Lambda)\ell z}|\beta\rangle, \tag{9}$$

which implies an extended version of the orthogonality relationship,

$$\langle\beta^*|\hat{B}e^{(-2\pi i/\Lambda)\ell z}|\beta'\rangle = 0 \tag{10}$$

for $\beta \neq \beta' + (2\pi/\Lambda)\ell$. Because of the equivalency of Eq. (9), it suffices to consider eigenvalues whose real parts are in the first Brillouin zone [1,37], i.e., $\Re[\beta] \in (-\pi/\Lambda, \pi/\Lambda]$.

Guided modes of a waveguide have finite spatial extent, and it follows that they have discrete eigenvalues β_n. We denote such states by $|n\rangle$ and normalize them to

$$\langle m^*|\hat{B}|n\rangle = \delta_{m,n}\eta_n, \tag{11}$$

where $|\eta_n| = 1$ and η_n is given by the phase angle of $\langle n^*|\hat{B}|n\rangle$, while $|m^*\rangle$ denotes the state with eigenvalue β_m^*. This corresponds to normalizing each real-β mode's time-averaged transmitted power to 1/4 [34]. In order to have a complete basis, one must generally include the continuum of nonguided states $|\beta\rangle$, which are typically normalized to delta functions: $\langle\beta^*|\hat{B}|\beta'\rangle = \delta(\beta - \beta')\eta_\beta$. We do not treat this continuum explicitly here, as the algebraic generalization is straightforward (sums over states become integrals); in fact, the continuum can be thought of as a limit of a discrete set of states with conducting boundary conditions that go to infinity. In any case, most numerical implementations of coupled-mode theory must employ a discrete set of states and a finite computational cell.

III. COUPLED-MODE THEORY FOR NONGRATED WAVEGUIDES

First, we review the well-known coupled-mode theory for nongrated waveguides in the instantaneous eigenmode (''quasimode'') basis [8,15,32], casting the notation and derivation in a quantum-mechanics-like form that prepares for the generalization of the following section. Consider an arbitrary $\varepsilon(z)$ [and/or $\mu(z)$, although we usually have $\mu=1$], where the xy dependence is implicit. At any z, one can define the instantaneous eigenstates $|n\rangle_z$ and eigenvalues $\beta_n(z)$ of an imaginary uniform waveguide with that cross section, satisfying

$$\hat{A}|n\rangle_z = \beta_n(z)\hat{B}|n\rangle_z . \tag{12}$$

As long as the cross section changes continuously, these are all continuous functions of z (perhaps only piecewise differentiable). The actual field $|\psi(z)\rangle$ can then be expanded in these states at each z,

$$|\psi(z)\rangle = \sum_n c_n(z)|n\rangle_z \exp\left(i\int^z \beta_n(z')dz'\right), \tag{13}$$

with z-varying coefficients $c_n(z)$. (The integrated phase choice [30] produces a convenient cancellation in the coupled-mode equations.) These coefficients satisfy a linear differential equation that can be found by substituting Eq. (13) into Maxwell's equations, i.e., into Eq. (1),

$$\begin{aligned} -i\frac{\partial}{\partial z}\hat{B}|\psi(z)\rangle &= \hat{B}\sum_n \left[-i\frac{dc_n}{dz}|n\rangle_z - ic_n\frac{\partial|n\rangle_z}{\partial z} + \beta_n c_n|n\rangle_z\right]\exp\left(i\int \beta_n\right) \\ &= \hat{A}|\psi(z)\rangle = \hat{B}\sum_n \beta_n c_n|n\rangle_z \exp\left(i\int \beta_n\right), \end{aligned} \tag{14}$$

where we have used Eq. (12). The equation for a given $\partial c_m/\partial z$ is then found by multiplying both sides by $\eta_m^*\langle m^*|_z\hat{B}$ and employing the orthonormality relation (11), which yields

$$\frac{dc_m}{dz} = -\eta_m^*\sum_n \left\langle m^*\left|\hat{B}\frac{\partial|n\rangle_z}{\partial z}\right.\right. \times\exp\left(i\int^z[\beta_n(z')-\beta_m(z')]dz'\right)c_n . \tag{15}$$

This is still not entirely convenient, as it requires the derivative of $|n\rangle_z$. The derivative of an eigenstate, however, is given *exactly* from first-order perturbation theory [32], and so one finds

$$\begin{aligned} \frac{dc_m}{dz} &= -\eta_m^*\sum_{n\neq m}\frac{\left\langle m^*\left|\frac{\partial\hat{A}}{\partial z}\right|n\right\rangle_z}{\beta_n(z)-\beta_m(z)} \\ &\quad\times\exp\left(i\int^z[\beta_n(z')-\beta_m(z')]dz'\right)c_n \\ &\quad -\eta_m^*\langle m^*|\hat{B}\frac{\partial|m\rangle_z}{\partial z}c_m . \end{aligned} \tag{16}$$

As described in Appendix B, this transformation can also be derived by differentiating the eigenequation, and the last term in Eq. (16) can usually be set to zero by a simple phase choice (e.g., making the real-β eigenstates purely real with a consistent sign). The z-varying coupling coefficients of this equation are now given in terms of the eigenstates of each cross section and the rate of change of the eigenoperator $\partial\hat{A}/\partial z$. This inner-product integral (over the cross section) can be written more simply in terms of the full six-component field state, after integration by parts in xy [34,35],

$$\left\langle m^*\left|\frac{\partial\hat{A}}{\partial z}\right|n\right\rangle = \frac{\omega}{c}\int\left[\frac{\partial\varepsilon}{\partial z}\mathbf{E}_{m^*}^*\cdot\mathbf{E}_n + \frac{\partial\mu}{\partial z}\mathbf{H}_{m^*}^*\cdot\mathbf{H}_n\right]. \tag{17}$$

The m^* and n subscripts denote the fields of $|m^*\rangle$ and $|n\rangle$, respectively. Note, however, that when the ε or μ variation includes shifting high-contrast boundaries, special care must be taken with this integral (and, in particular, with the resulting surface integrals) because of the field discontinuities [34–36].

Equation (16) is of precisely the same form in quantum mechanics, and exactly the same methods and theorems apply. In particular, in the limit where the cross-sectional variation becomes arbitrarily slow (and thus $\partial\hat{A}/\partial z$ becomes small), the well-known adiabatic theorem [8,38–43], recapitulated in Appendix A, states that $c_n(z)$ goes to $c_n(0)$—no intermodal scattering occurs. (We discuss approximations for the intermediate case of finite slow tapers in Sec. IV E, once we have developed the generalized theory.)

IV. COUPLED-MODE THEORY FOR GRATED WAVEGUIDES

Above, the key to deriving a coupled-mode theory with near-adiabatic coefficients was the identification of a slowly varying ''instantaneous'' waveguide at any given z. That is, at each z we imagined an infinite, uniform waveguide and its eigenmodes. The same idea carries over to gratings, except that here we imagine an instantaneous, infinite, *periodically grated* waveguide. Because this instantaneous grated waveguide has axial variation, we must explicitly identify a *virtual* coordinate $\tilde{z}$ in which the instantaneous waveguide extends infinitely, distinct from the *physical* coordinate z of a given cross section, as depicted in Fig. 1 and discussed in more detail below. This extension into a virtual coordinate system causes the algebra to be somewhat more interesting

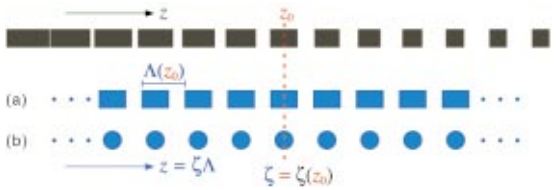

FIG. 1. (Color) For a physical nonuniform grating (top, black) at a given $z=z_0$, we imagine (a) an infinite uniform grating with pitch $\Lambda(z_0)$ extending in a virtual $\tilde{z}$ space, matching the physical cross section at corresponding scaled coordinates $\tilde{z}/\Lambda=\tilde{\zeta}=\zeta(z_0)$. Such a grating is not unique, and corresponds to a choice of basis—an alternate choice that also matches the requisite cross section is shown in (b).

than before, but we shall see that we arrive at almost exactly the same form for the result.

Moreover, the instantaneous grating has a period $\Lambda(z)$ that may be z dependent (e.g., for a ''chirped'' grating), as described below. This makes it convenient to introduce the scaled virtual coordinate $\tilde{\zeta}\equiv\tilde{z}/\Lambda(z)$ so that the instantaneous gratings always have unit period. We must also define a corresponding ''physical'' scaled coordinate $\zeta\equiv\int^z dz'/\Lambda(z')$; intuitively, ζ is the number of variable periods traversed up to z. (The proper coordinate choice is critical to obtain a convenient form for the coupled-mode equations.)

A. The instantaneous virtual grating

Given our physical variation $\varepsilon(z)$ (again leaving the xy variation implicit and dropping μ for simplicity), we must define at every z a virtual unit-periodic grating $\varepsilon_z(\tilde{\zeta})$, where $\varepsilon_z(\tilde{\zeta}+1)=\varepsilon_z(\tilde{\zeta})$. The connection to the physical system is that we require

$$\varepsilon_z(\zeta)=\varepsilon(z). \tag{18}$$

That is, the virtual grating must coincide with the physical waveguide cross section at $\tilde{\zeta}=\zeta$ (the analog to z in the virtual space); this also implies a choice of origin in virtual space. Because $\varepsilon_z(\tilde{\zeta})$ is defined by the entire $\tilde{\zeta}\in[0,1)$ primitive cell, but is only constrained at a single $\tilde{\zeta}$, the choice of the instantaneous waveguide ε_z and $\Lambda(z)$ is *not unique* as shown in Fig. 1, unlike in the preceding section. This merely indicates a choice of expansion bases, however, and for good adiabaticity we should select ε_z and $\Lambda(z)$ so that they vary continuously and as slowly as possible with z.

Figure 1 points out that the virtual grating need not even resemble the physical structure in order to satisfy Eq. (18), but the more similar the physical and virtual structures are, the more adiabatic the basis choice is likely to be. Another example that directly illustrates the consequences of the choice of virtual grating is depicted in Fig. 2. Here, we imagine a taper to a grated waveguide of pitch $\Lambda=1$, consisting of blocks of width $w=w_f$, from a uniform waveguide (corresponding to $w=1$), an example considered in more detail in Sec. V. The natural virtual waveguides are grated waveguides with blocks of intermediate widths $w(z)$ ranging

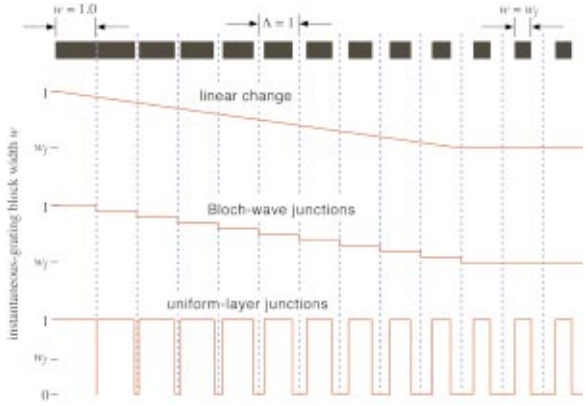

FIG. 2. (Color) The same (constant-pitch) physical taper, from a uniform waveguide to a grated waveguide of blocks with width $w=w_f$, can be represented by different virtual tapers $w(z)$: (top) a continuous linear change; (middle) sharp junctions at each Λ of uniform grated waveguides; (bottom) sharp junctions of uniform waveguides given by the instantaneous cross section (traditional coupled-mode theory).

from 1 to w_f, but many choices of $w(z)$ lead to exactly the same physical taper structure. The most adiabatic choice is a linear variation, shown as the top graph of the figure. Another possibility is a piecewise-constant sequence of uniform grated waveguides, changing discontinuously after each period; this case, shown in the middle graph, leads to a scattering-matrix formulation based on the transfer matrices at each junction (a generalization of Ref. [19]). A third choice is that of *uniform* waveguides ($w=1$ or $w=0$), just as in the traditional theory of Sec. IV above; this will lead to the standard a set of transfer matrices at each z interface. All of these representations will produce the *same* numerical result for the transmission, if integrated with a complete basis, but are different basis choices that will have different (stronger or weaker) scattering between the basis coefficients. The first choice of a linear change is the best from an adiabatic perspective, producing a continuous set of differential equations (below) that can be integrated efficiently with few basis functions for slow tapers; the third choice is the worst, involving strong scattering even for a uniform grating and requiring a large basis for accurate results.

Once a virtual grating $\varepsilon_z(\tilde{\zeta})$ is chosen at each z, we find its Bloch eigenfunctions $|n(\tilde{\zeta})\rangle_z$, where we explicitly identify the virtual $\tilde{\zeta}$ dependence inside the brackets, as opposed to the variation with z as the instantaneous grating changes, denoted by the subscript. This eigenfunction satisfies

$$\hat{C}_z(\tilde{\zeta})|n(\tilde{\zeta})\rangle_z\equiv\left(\hat{A}_z(\tilde{\zeta})+\frac{i}{\Lambda(z)}\frac{\partial}{\partial\tilde{\zeta}}\hat{B}\right)|n(\tilde{\zeta})\rangle_z$$

$$=\beta_n(z)\hat{B}|n(\tilde{\zeta})\rangle_z, \tag{19}$$

where $\hat{A}_z(\tilde{\zeta})$ is the $\hat{A}$ from Eq. (3) with $\varepsilon_z(\tilde{\zeta})$ instead of ε [so that $\hat{A}_z(\zeta)=\hat{A}$)], and we have defined a new operator $\hat{C}_z(\tilde{\zeta})$ in analog to Eq. (8). As described earlier, we only consider eigenfunctions in the first Brillouin zone, $\Re[\beta]$

$\in(-\pi/\Lambda,\pi/\Lambda]$, where $\Re$ denotes the real part, since other modes are redundant (and are effectively reinserted below).

B. A parametrized expansion basis

The question now is how to turn these eigenfunctions into an expansion basis for the state $|\psi(z)\rangle$. We would like to expand in $|n(\zeta)\rangle_z$, i.e., the $\tilde{\zeta}=\zeta(z)$ slice of the instantaneous eigenstate at z, since this is the *exact* Bloch eigenstate basis in the limit of a uniform grating [where $\zeta=z/\Lambda$ and $|n(\zeta)\rangle_z$ is the eigenstate $|n\rangle$]. In that basis, however, we no longer have a separate $\tilde{\zeta}$ dependence, and this is a problem: in order to employ the orthonormality relation to pick out particular state coefficients (as in Sec. III), we must integrate over $\tilde{\zeta}$ and *not* over ζ (and z). (Equivalently, the Bloch basis is *overcomplete* on a single cross section/slice, unlike the conventional instantaneous basis of Sec. III, and must be disambiguated.)

We must therefore add an explicit $\tilde{\zeta}$ dependence back into the basis, and we do this by extending the coupled-mode equations to solve a *family* of problems parametrized by shifts in the virtual gratings. At the end, we will project back down to the physical problem to yield the desired result in the $|n(\zeta)\rangle_z$ basis.

In particular, consider the state $|n(\zeta+\tilde{\zeta})\rangle_z$, which solves the eigenproblem of Eq. (19) for the operator $\hat{A}_z(\zeta+\tilde{\zeta})$ in $\varepsilon_z(\zeta+\tilde{\zeta})$ [with the same eigenvalue $\beta_n(z)$]. Up to now, we have imagined that for each z, we have a virtual grating in $\tilde{z}$ space—z parametrizes the $\tilde{z}$ gratings. The converse is also possible, however: for every $\tilde{\zeta}$, $\varepsilon_z(\zeta+\tilde{\zeta})$ as a function of z is a different variable-grating structure, coinciding with our physical system $\varepsilon(z)$ only for the shift $\tilde{\zeta}=0$ (*not* $\zeta=0$). For *each* of these systems, parametrized (periodically) by $\tilde{\zeta}$, we can imagine solving for the field evolution $|\psi(z)\rangle_{\tilde{\zeta}}$, expanding the fields at z in the basis of $|n(\zeta+\tilde{\zeta})\rangle_z$,

$$|\psi(z)\rangle_{\tilde{\zeta}}=\sum_n c_n(z,\tilde{\zeta})|n(\zeta+\tilde{\zeta})\rangle_z \exp\left(i\int^z \beta_n(z')dz'\right). \tag{20}$$

Because the $\tilde{\zeta}$ coordinate is unit periodic, we can choose $c_n(z,\tilde{\zeta}+1)=c_n(z,\tilde{\zeta})$, and thus the c_n can be expanded as a Fourier series in $\tilde{\zeta}$,

$$c_n(z,\tilde{\zeta})=\sum_\ell c_{n,\ell}(z)e^{-2\pi i\ell\tilde{\zeta}} \tag{21}$$

for some coefficients $c_{n,\ell}(z)$. The physical $\tilde{\zeta}=0$ solution is then simply $c_n(z)=\Sigma_\ell c_{n,\ell}(z)$.

C. Coupled-mode equations

To solve for the parametrized field evolution, we substitute $|\psi(z)\rangle_{\tilde{\zeta}}$ into Maxwell's equations (1) for $\varepsilon_z(\zeta+\tilde{\zeta})$,

$$\begin{aligned}-i\frac{\partial}{\partial z}\hat{B}|\psi(z)\rangle_{\tilde{\zeta}}&=\hat{B}\sum_n\left[-i\frac{dc_n}{dz}|n\rangle_z-ic_n\frac{\partial|n\rangle_z}{\partial z}\right.\\&\left.-\frac{i}{\Lambda}c_n\frac{\partial}{\partial\tilde{\zeta}}|n\rangle_z+\beta_nc_n|n\rangle_z\right]e^{i\int\beta_n}\\&=\hat{A}_z(\zeta+\tilde{\zeta})|\psi(z)\rangle_{\tilde{\zeta}}\\&=\hat{B}\sum_n\left[-\frac{i}{\Lambda}c_n\frac{\partial}{\partial\tilde{\zeta}}|n\rangle_z+\beta_nc_n|n\rangle_z\right]e^{i\int\beta_n},\end{aligned} \tag{22}$$

where $|n\rangle_z$ denotes $|n(\zeta+\tilde{\zeta})\rangle_z$, and $\partial|n\rangle_z/\partial z$ is the partial derivative with respect to the z subscript *only* (not acting on $\zeta+\tilde{\zeta}$). [We have used the fact that $(d/dz)f_z(\zeta+\tilde{\zeta})=(\partial/\partial z)f_z(\zeta+\tilde{\zeta})+(1/\Lambda(z))(\partial/\partial\tilde{\zeta})f_z(\zeta+\tilde{\zeta}).$] Just as in Sec. III, several terms cancel due to our choice of eigenstate basis (and the proper coordinate system). Given the remaining terms, we can find the equation for $dc_{m,k}/dz$ by multiplying with $\eta_m^*\langle m^*(\zeta+\tilde{\zeta})|_z e^{2\pi ik\tilde{\zeta}}\hat{B}$, which involves an integral over $\tilde{\zeta}$—that is, we must integrate over the *family* of field solutions at a fixed z. The generalized orthonormality relation of Eq. (10) thereby yields

$$\begin{aligned}\frac{dc_{m,k}}{dz}=-\eta_m^*\sum_{n,\ell}\left\langle m^*(\zeta+\tilde{\zeta})\right|\hat{B}e^{-2\pi i(\ell-k)\tilde{\zeta}}\frac{\partial|n(\zeta+\tilde{\zeta})\rangle_z}{\partial z}\\\times\exp\left(i\int^z[\beta_n(z')-\beta_m(z')]dz'\right)c_{n,\ell}.\end{aligned} \tag{23}$$

Here, the inner-product integral is over the virtual coordinate $\tilde{\zeta}$ shifted by ζ; we can eliminate this z dependence by the coordinate change $\tilde{\zeta}\to\tilde{\zeta}-\zeta$,

$$\begin{aligned}\frac{dc_{m,k}}{dz}=-\eta_m^*\sum_{n,\ell}\langle m^*|\hat{B}e^{-2\pi i(\ell-k)\tilde{\zeta}}\frac{\partial|n\rangle_z}{\partial z}\\\times\exp\left(2\pi i(\ell-k)\zeta+i\int(\beta_n-\beta_m)\right)c_{n,\ell},\end{aligned} \tag{24}$$

where $|m^*\rangle_z$ and $|n\rangle_z$ *now* denote simply $|m^*(\tilde{\zeta})\rangle_z$ and $|n(\tilde{\zeta})\rangle_z$. Finally, we employ the method of the Appendix B, as in Sec. III, to re-express $\partial|n\rangle_z/\partial z$ in terms of the derivative of the eigenoperator from Eq. (19),

$$\begin{aligned}\frac{dc_{m,k}}{dz}=-\eta_m^*\sum_{n,\ell\neq m,k}\frac{\left\langle m^*\right|e^{2\pi ik\tilde{\zeta}}\frac{\partial\hat{C}_z(\tilde{\zeta})}{\partial z}e^{-2\pi i\ell\tilde{\zeta}}\left|n\right\rangle_z}{\Delta\beta_{n,\ell;m,k}(z)}\\\times\exp\left(i\int^z\Delta\beta_{n,\ell;m,k}(z')dz'\right)c_{n,\ell}\\-\eta_m^*\langle m^*|\hat{B}\frac{\partial|m\rangle_z}{\partial z}c_{m,k},\end{aligned} \tag{25}$$

where the phase mismatch $\Delta\beta$ is given by

$$\Delta\beta_{n,\ell;m,k}(z) \equiv \beta_n(z) - \beta_m(z) + \frac{2\pi}{\Lambda(z)}(\ell - k) \qquad (26)$$

and $\partial\hat{C}_z(\tilde{\zeta})/\partial z$ is

$$\frac{\partial\hat{C}_z(\tilde{\zeta})}{\partial z} = \frac{\partial\hat{A}_z(\tilde{\zeta})}{\partial z} + i\frac{d\Lambda^{-1}}{dz}\hat{B}\frac{\partial}{\partial\tilde{\zeta}}. \qquad (27)$$

As discussed in Appendix B, the final $\langle m^*|\hat{B}\partial/\partial z|m\rangle_z$ "self-interaction" term can be set to zero (at least for any real-β mode) by an appropriate phase choice for the eigenstates $|m\rangle_z$, and we therefore drop it in most of the the following discussion.

In deriving the numerator of Eq. (25), we have used the fact that the commutator of $e^{-2\pi i\ell\tilde{\zeta}}$ with $\partial/\partial\tilde{\zeta}$ is a constant, which integrates to zero thanks to the orthonormality relation—so, we are free to move the phase terms to either side of $\partial\hat{C}_z(\tilde{\zeta})/\partial z$. We have also used Eq. (9) in order to interpret the combination of the phase terms with the eigenstates $|n\rangle_z$ and $|m\rangle_z$ as the eigenstates of $\beta_n + 2\pi\ell/\Lambda$ and $\beta_m + 2\pi k/\Lambda$. Note that in the limit of $d\Lambda^{-1}/dz = 0$ and $\Lambda \to 0$, we reproduce the standard result of Sec. III.

D. The adiabatic theorem

The generalized coupled-mode equation of Eq. (25) can be simply understood as the ordinary coupled-mode equations in the basis of the Bloch states plus all of their $2\pi/\Lambda$ equivalents. There are only a few new aspects, mainly: (i) the inner product is over the three-dimensional (3D) unit cell in $\tilde{\zeta}$ space, not over the cross section; (ii) there is an additional term from the rate of change $d\Lambda/dz$ of the period; and (iii) the k label is "fictitious," and must be summed at the end via Eq. (21). None of these variations affects the proof of the adiabatic theorem (e.g., in Appendix A), which only depends on the basic form of the system of equations and on the decreasing coupling as the system changes more slowly, so we can immediately conclude that it holds here as well: If the system changes arbitrarily slowly with z and β_n remains real (propagating) and discrete (guided), the *Bloch* modes transform adiabatically and $c_n(z)$ approaches $c_n(0)$. The key conditions that the mode always be propagating and guided are discussed in further detail in Sec. VI, where we show how they can be satisfied by computing the band diagrams of all intermediate points in the taper and altering the taper design accordingly.

E. Approximations for slow tapers

Solving the coupled-mode equations in general, for finite tapers, involves setting boundary conditions on the incoming waves at both ends of a waveguide segment and then integrating the full coupled-mode system [8,15], in principle, requiring expansion in infinitely many modes and k values. For slowly varying systems, however, several simplifications apply. First, it is clear from Eq. (25) that nearby-β modes give the greatest contribution, so the basis can be truncated. Second, for near-adiabatic evolution starting with power in a single mode, $c_{m,k}(0) = \delta_{m,n}\delta_{k,0}c_n(0)$ [55], one can integrate the equations *approximately*, to first order in $\partial\hat{C}_z/\partial z$,

$$c_{m\neq n}(z_0) \cong -c_n(0)\,\eta_m^* \int_0^{z_0} dz \sum_k \frac{\left\langle m^* \left| e^{2\pi ik\tilde{\zeta}} \frac{\partial\hat{C}_z(\tilde{\zeta})}{\partial z} \right| n \right\rangle_z}{\Delta\beta_{n,0;m,k}(z)} \times \exp\left(i\int_0^z \Delta\beta_{n,0;m,k}(z')dz' \right), \qquad (28)$$

with $|c_m|^2/|c_n|^2$ being the scattered power fraction; this approximation should be accurate as long as the total scattered power is small (e.g., <0.1 is often sufficient). The lowest-order losses in mode n are then found by conservation of power: $|c_n(z)|^2 = |c_n(0)|^2 - \Sigma_{m\neq n}|c_m(z)|^2$. This technique works even to compute reflections: if c_{-m} denotes a backward-propagating wave, then the boundary condition of $c_{-m}(z_0) = 0$ at the end of a taper can be satisfied to first order by setting the reflected wave $c_{-m}(0)$ equal to -1 times the $c_{-m}(z_0)$ computed from Eq. (28).

In single-mode grated waveguides (e.g., in photonic crystals), the scattering losses for slow tapers will often be completely dominated by reflection, for several reasons. First, in an omnidirectional photonic crystal, there are no other propagating states in the band gap to couple to; this not true, however, for transitions between photonic crystals and conventional waveguides. Second, if one operates near the guided-band edge, the smallest $\Delta\beta$ will typically be for the reflected mode (which lies just on the other side of the band edge). Third, recall that the fields in the coupling-coefficient integrals are normalized—equivalently, one divides the coefficients by $|\langle n^*|\hat{B}|n\rangle|$ terms, which are proportional to the power and thus to the energy density times the group velocity. The group velocity in a photonic crystal, however, is often small due to Bragg scattering (going to zero at the band edge), and thus the coupling to reflected modes (which are also slow) can be greatly amplified (inversely with the group velocity) relative to, e.g., radiating modes (above the light line). We demonstrate this domination of reflection numerically in Sec. V, and its fortunate consequence is that one typically only needs to compute the scattering from Eq. (28) between a *single pair* of guided modes.

One can gain additional insight from this first-order approximation because the coupling coefficients and $\Delta\beta$ values are usually slowly varying. As a crude simplification, suppose that we simply replace them by *constants*: their values at some intermediate point in the taper. Furthermore, consider only the k with the largest contribution, i.e., the k for which $|\Delta\beta_{n,0;m,k}|$ is minimum. In this case, Eq. (28) can be integrated analytically to yield a scattered power,

$$\frac{|c_{m\neq n}(z)|^2}{|c_n(0)|^2} \approx 4\left| \frac{\overline{\langle m^*|e^{2\pi ik\tilde{\zeta}}\frac{\partial\hat{C}_z}{\partial z}|n\rangle}}{\overline{\Delta\beta_{nm}}^2} \right|^2 \sin^2(\overline{\Delta\beta_{nm}}z/2), \qquad (29)$$

where the bar above the $\overline{\Delta\beta_{nm}}$, etc., indicates whatever average/intermediate value is chosen. Such an approximation actually works surprisingly well to predict the qualitative behavior of a taper with a large taper length $z=L$: as we demonstrate in Sec. V, the scattering as a function of L oscillates sinusoidally with period $\sim 2\pi/\Delta\beta$ and overall decreases as $1/L^2$ (from the taper rate $\partial\hat{C}_z/\partial z \sim 1/L$).

F. Coupling-factor evaluation

The coupling factor, i.e., the $\partial\hat{C}_z(\tilde{\zeta})/\partial z$ inner product in Eqs. (25),(28), can be expressed in a derivative-free form that is more convenient to evaluate. First, the $\hat{B}\partial/\partial\tilde{\zeta}$ term in Eq. (27) can be rewritten in terms of $\hat{A}_z$ and a constant term (which integrates to zero) via the eigenequation (19). Second, as in Sec. III and Refs. [34,35], we can integrate by parts in xy to yield an integral (over the $\tilde{\zeta}$ unit cell) in terms of the full six-component fields of the instantaneous Bloch states at z,

$$\begin{aligned}\left\langle m^*\left| e^{2\pi ik\tilde{\zeta}}\frac{\partial\hat{C}_z(\tilde{\zeta})}{\partial z}\right| n\right\rangle_z &= \frac{\omega}{c}\int e^{(2\pi i/\Lambda)k\tilde{z}}\left[\left(\frac{\partial\varepsilon_z(\tilde{\zeta})}{\partial z}-\frac{d\Lambda^{-1}}{dz}\varepsilon_z\right)\mathbf{E}^*_{m^*}\cdot\mathbf{E}_n\right.\\ &\quad +2\frac{d\Lambda^{-1}}{dz}\varepsilon_z E^*_{m^*,\tilde{z}}E_{n,\tilde{z}}\\ &\quad +\left(\frac{\partial\mu_z(\tilde{\zeta})}{\partial z}-\frac{d\Lambda^{-1}}{dz}\mu_z\right)\mathbf{H}^*_{m^*}\cdot\mathbf{H}_n\\ &\quad \left.+2\frac{d\Lambda^{-1}}{dz}\mu_z H^*_{m^*,\tilde{z}}H_{n,\tilde{z}}\right]dxdyd\tilde{z},\end{aligned}\tag{30}$$

where we have recast the integral in terms of the unscaled $\tilde{z}$ coordinate, and have included the generalization of $\mu\neq 1$ and an instantaneous μ_z grating analogous to ε_z. (The fields are assumed to be normalized, $\langle n^*|\hat{B}|n\rangle_z=\eta_n$, which cancels the $\tilde{\zeta}\to\tilde{z}$ Jacobian factor Λ as long as we are consistent.) The m^* and n subscripts, as before, denote the fields of $|m^*\rangle$ and $|n\rangle$. Again, $\partial\varepsilon_z(\tilde{\zeta})/\partial z$ (or $\partial\mu_z(\tilde{\zeta})/\partial z$) must be handled specially for moving boundaries in high-contrast systems—there, they yield well-defined surface integrals involving only the continuous $\mathbf{E}_\parallel$ and $D_\perp$ (or $\mathbf{H}_\parallel$ and $B_\perp$) field components at the boundaries [36]. We also note that Eq. (30) involves $\partial\varepsilon_z(\tilde{\zeta})/\partial z|_{\tilde{\zeta}=\tilde{z}/\Lambda}$, *not* $\partial\varepsilon_z(\tilde{z})/\partial z$ (similarly for μ_z): it is the rate of change of the *unit-period* virtual grating.

In order to drop the inconvenient $\langle n^*|\hat{B}(\partial/\partial z)|n\rangle_z$ self-interaction term from the coupled-mode equations, as described in Appendix B, we must choose a consistent phase for the eigenstates as a function of z. As described in the Appendix, there are several ways to enforce such phase consistency in practice, the simplest being in the common case where the dielectric structure has inversion symmetry, in which case the Fourier transform can be chosen as purely real with a canonical sign. Finally, as described below, because the coupling factors are continuous functions of z, it suffices to compute them only at a few intermediate points and then interpolate.

V. NUMERICAL EXAMPLE

Despite the contortions of the derivation, our end result (25) is straightforward to apply: a set of coupled differential equations in the Bloch eigenmodes with z-varying coefficients. A key feature is that once these coupling coefficients are computed for a given taper length L, with a computation involving only the *unit cells* of intermediate virtual waveguides, they can then be reapplied to any L (any degree of gradation) by scaling them with the rate of change. Unlike most numerical methods, the computation becomes easier and smaller as the taper becomes *more* gradual, since fewer basis functions are required for accuracy in the adiabatic limit. To illustrate this, we apply the coupled-mode equations above to a waveguide transition in an example two-dimensional system, depicted with their dispersion relations in Fig. 3: a conventional dielectric waveguide ($\varepsilon=12$, thickness $h=0.4a$) and a grated waveguide consisting of a sequence of $w\times h=0.4a\times 0.4a$ blocks ($\varepsilon=12$, period $\Lambda=a$), both surrounded by air ($\varepsilon=1$). We focus on the fundamental TM-polarized modes of each waveguide, for which $\mathbf{E}=E\hat{\mathbf{y}}$ is perpendicular to the 2D ($x-z$) plane and the field is even with respect to the $x=0$ waveguide axis. The modes in both waveguides are confined in the lateral (x) direction by index-guiding (they lie beneath the light line), and the grated waveguide has a band gap in its guided modes [44]. We emphasize that our theory is fully three dimensional; it is only the limitations of the second numerical method that we use here for comparison that limits us to two dimensions (other 3D methods typically require enormous computing power to calculate transmission through very gradual tapers).

A. Computational methods

In order to compute the eigenmodes of these waveguides (and of the intermediate instantaneous gratings in the tapers), we employ preconditioned conjugate-gradient minimization of the block Rayleigh quotient for the fully vectorial Maxwell's equations in a plane wave basis with a lateral (x) supercell, using a freely available software package [45]. (This technique yields the frequency ω for a given β, but that relation was inverted using Newton's method [46] with the help of the group velocity $d\omega/d\beta$ computed via the Hellman-Feynman theorem [32].) The eigenmodes were then used to compute the coupling constants by Eq. (30), modified for shifting boundaries as in Ref. [36]. All structures possess inversion symmetry, allowing the field Fourier transforms to be taken as purely real [45] so that phase consistency (as described in Appendix B) is maintained by a simple choice of sign.

Coupling constants and eigenvalues β were thereby computed for 17 intermediate waveguides in the taper, linearly interpolated, and integrated by a trapezoidal rule. To integrate the full coupled-mode equations, in principle, one would employ a set of many guided, evanescent, and radia-

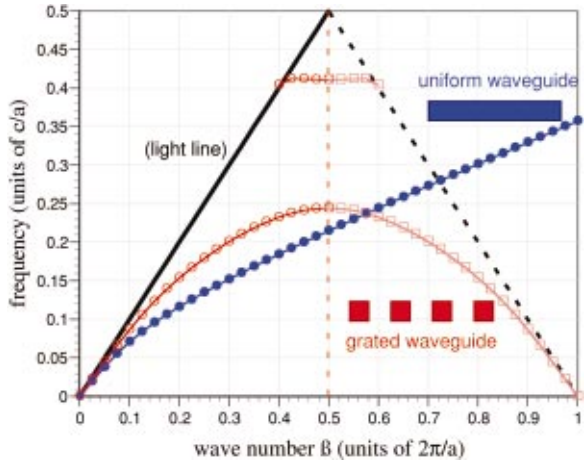

FIG. 3. (Color) Dispersion relation for a 2D uniform dielectric waveguide (filled blue circles) and a grated waveguide consisting of a sequence of blocks (hollow red symbols), with the structures shown as insets. The grated waveguide is periodic in β, with the periodic extension of the backward-propagating modes shown (squares) after the dashed vertical line. Only TM-polarized (**H** in plane) modes having even symmetry with respect to the waveguide axis are shown.

tion modes (above the light line). Here, however, we focus on modes in the vicinity of the band gap where photonic-crystal effects are strongest (and therefore of the greatest interest), so the primary coupling is to the reflected mode as discussed in Sec. IV E. Moreover, since we desire mainly to achieve high transmission—i.e., near-adiabatic transitions—we employ the first-order integration (with respect to the taper rate) approximation of Eq. (28). In this way, we need only compute the coupling-matrix elements between the incident $(+\beta)$ and reflected $(-\beta)$ modes, as well as the various $2\pi k/\Lambda$ shifts; we found $k=$

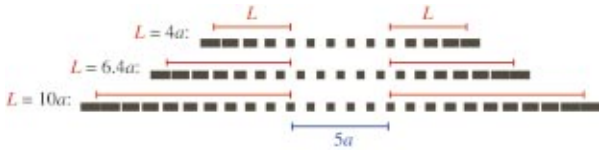

FIG. 4. (Color) Three constant-period ($\Lambda=a$) linear tapers between a uniform waveguide and a grated waveguide of dielectric squares, and back again after five periods of uniform grating. Taper lengths L of $4a$, $6.4a$ (yielding an asymmetric on/off taper), and $10a$ are shown.

$\{-1,0,1,2,3\}$ to be more than sufficient [$k=1$ gives the smallest $\Delta\beta=\beta-(-\beta)-2\pi k/\Lambda$ for β near π/Λ, and is thus the largest contribution]. Moreover, once the coupling matrix elements are calculated, the scattered/reflected power can be found for many taper rates at a negligible added computational cost.

For comparison with the coupled-mode theory, we employed a rigorous scattering (transfer) matrix method based on eigenmode expansions at each cross section [18] and lateral perfectly matched layer boundary conditions [47], with a freely available software implementation [21,48]. Given an incident field in the fundamental mode of a uniform (nongrated) waveguide, this method returns the transmitted and reflected power in any desired modes of uniform input and/or output waveguides. Moreover, if the input and output waveguides are z-uniform waveguides, this method induces zero numerical reflections from those two boundaries.

Therefore, because of the limitations of this scattering-matrix method, we compute the transmission through a *double taper*: starting with the uniform waveguide, transitioning to the grated waveguide, propagating for five uniform periods, and then transitioning symmetrically back to the uniform waveguide. This is done for both the ''exact'' scattering-matrix method and for the first-order integration of

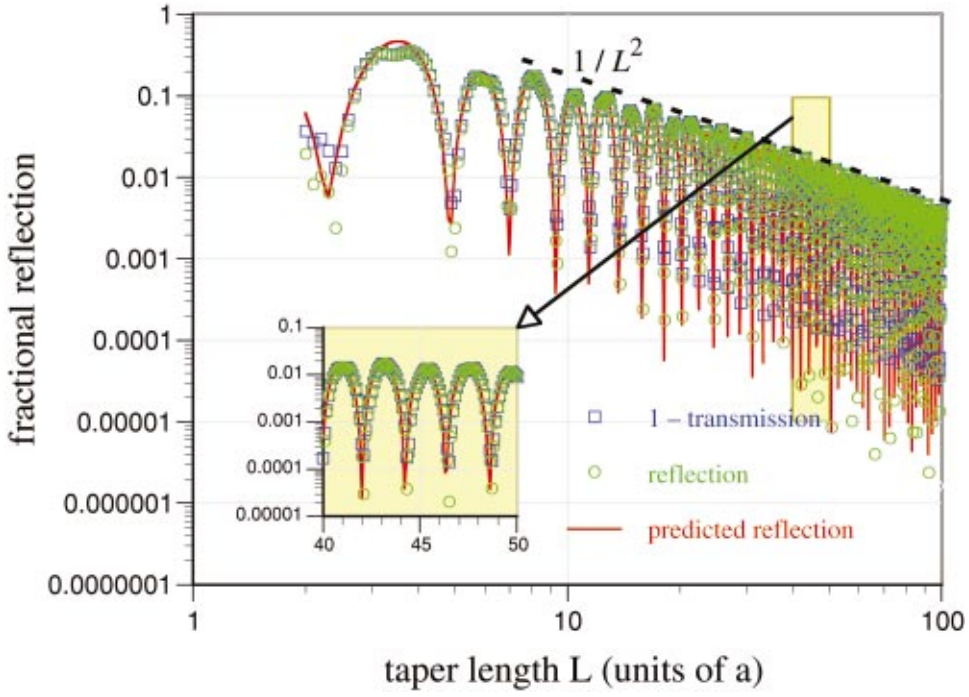

FIG. 5. (Color) Reflected power at $\omega=0.2\times 2\pi c/a$ from the constant-period tapers of Fig. 4 as a function of taper length L. ''Exact'' scattering-matrix results are shown as green circles, while the solid red line is the prediction of our coupled-mode theory with the first-order approximation. Blue squares are one minus the transmission from the scattering-matrix calculation, and demonstrate that the transmission losses are dominated by reflections except for $L<3a$. The inset is a magnified view for $L=40\cdots 50a$, showing the typical picture in the slow-taper limit.

the coupled-mode equations, in order to compare the reflection coefficients (power into the fundamental backward-propagating mode of the input waveguide). Because of the proximity of the band edge, such reflections completely dominate the losses—as seen below, the sum of transmitted/reflected power into the fundamental output/input mode was unity to within numerical accuracy for most taper lengths.

B. A constant-period taper

As a first example, we make a transition between the two waveguides by linearly varying the width w of the blocks, from $w=1.0a$ for the uniform waveguide to $w=0.4a$ for the grated waveguide, maintaining a constant pitch $\Lambda=a$, operating at a frequency of $\omega=0.2\times 2\pi c/a$. One could choose the physical tapered waveguide structure $\varepsilon(z)$ and then define a corresponding set of virtual instantaneous gratings $\varepsilon_z(\tilde{z})$, but it was more convenient to do the reverse: choose a continuously varying virtual grating and then define the physical structure by Eq. (18). Specifically, we choose the virtual grating $\varepsilon_z(\tilde{z})$ to have blocks with a width $w(z)/\Lambda = 1-0.6z/L$ (i.e., linearly varying) in the taper region of length L. In order to find the corresponding physical structure $\varepsilon(z)$, we must determine the block boundaries. The leading/trailing edge of the nth block in the (uniform) virtual grating is at $\tilde{z}_n^{\pm}(z)=n\pm w(z)/2\Lambda$, so by Eq. (18) the physical leading/trailing edge is at $z_n^{\pm}$, satisfying

$$\tilde{z}_n^{\pm}(z_n^{\pm}) \equiv n \pm w(z_n^{\pm})/2\Lambda = \zeta(z_n^{\pm}) \equiv z_n^{\pm}/\Lambda, \qquad (31)$$

which is an easily solved linear equation. This results in the taper structures shown in Fig. 4 for three different values of L; note that by defining the physical structure in this way, we are not limited to integer values of L/Λ (with fractional values causing asymmetric on/off tapers).

The resulting reflected power into the fundamental mode, shown in Fig. 5 shows excellent agreement between the scattering-matrix calculation and first-order coupled-mode theory, even for fairly short tapers. Also plotted is one minus the transmission, to verify that the sum of reflection and transmission is unity to numerical accuracy except for very short ($L<3a$) tapers, as is expected in the vicinity of the photonic band edge. Moreover, the curve exhibits the features that one can predict from the even cruder approximation of constant coupling in Eq. (29): the power oscillates with a period on the same order as $2\pi/\overline{\Delta\beta}\cong 4a$ and overall declines as $1/L^2$ towards the adiabatic limit of 100% transmission. Note that the phase of the oscillation is frequency dependent, much like a Fabry-Perot resonance oscillation, so in order to obtain a broad bandwidth of high transmission one should ideally choose a taper long enough so that the *maxima* of these oscillations are within tolerable levels.

In the following section, we compute a similar illustration of coupled-mode theory for the case of a variable-period taper, which is introduced in order to counter one common stumble in designing adiabatic grating tapers: a shifting band gap.

VI. PITFALLS TO AVOID

In designing adiabatic tapers, there are two ways in which the most straightforward transitions can actually *worsen* transmission, but which are easily circumvented if one is aware of them. These pitfalls are related to the two criteria for adiabatic tapers given in the introduction, and we illustrate both the problems and their solutions in this section.

A. Shifting band gaps

The first pitfall is that, when one operates near a band edge, a straightforward taper will often shift the band gap over the operating frequency, violating the conditions on the adiabatic theorem and with disastrous results for transmission. This case is easily detected by computing the band gaps of the intermediate points in the grating, and avoided by tapering the *period* as well as the grating strength in order to move the band gap out of the way. (A similar idea was previously demonstrated, without proof, for one-dimensional photonic crystals [13].)

The transition from a grated waveguide to a uniform waveguide in the preceding section, for example, exhibits precisely this problem. Not only does the gap reduce in size as the grating weakens, but it also shifts *down* in frequency because the uniform waveguide has more high-index material [1]. The instantaneous band-gap edges as a function of taper position are shown in Fig. 6 (blue circles), and illustrate this phenomenon. Now, if one operates at a frequency of $\omega=0.23\times 2\pi c/a$, for example (just below the lower band edge of the final grated waveguide), there will be a region of the taper where this frequency lies within the instantaneous band gap, causing the transmission to drop exponentially and to therefore *fall* as the taper becomes *more* gradual—this is shown in Fig. 7, computed via the scattering-matrix method. (There is a 56% resonance peak at a short taper length, but this will not yield a broad bandwidth.)

To correct the problem, one merely needs to shift the band gap back up, and this can be accomplished by reducing the pitch Λ. Here, we choose to keep $w=0.4a$ fixed and decrease $1/\Lambda$ linearly from $1/0.4a$ to $1/a$ to taper from the uniform waveguide to the grated waveguide. The resulting band gap edges are depicted in Fig. 6 (red squares): the band gap moves quickly upward now as the gap closes. Thus, the adiabatic theorem holds and the reflection eventually falls off as $\sim 1/L^2$; this is illustrated in Fig. 8. (As in the preceding section, the sum of the reflection and transmission is nearly unity.) In this figure, we compare the exact scattering-matrix result to our first-order coupled-mode theory, this time with a variable $\Lambda(z)$, and show that again it achieves accurate results once the taper is sufficiently long that the reflection is small (<0.1).

As with the constant-period taper, it was convenient to define our variable-period taper by first choosing the instantaneous gratings (to vary linearly), and then constructing the physical grating $\varepsilon(z)$ by applying Eq. (31). This time, $\zeta(z) = \int^z dz'/\Lambda$ is quadratic, so solving for the taper's block edges involves a quadratic equation. We should also note that, although w here is constant, w/Λ is not, so when evaluating the coupling matrix element of Eq. (30) there is still a

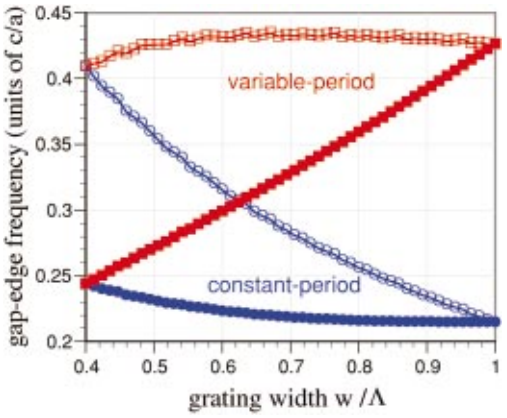

FIG. 6. (Color) The instantaneous band-gap edges as a function of fractional grating width w/Λ in the taper. Blue circles: fixed Λ, in which case the gap shifts down as it closes. Red squares: decreasing Λ (so that w is fixed), making the gap shift up as it closes. Any frequency that intersects the gap at any point in the taper will have low transmission.

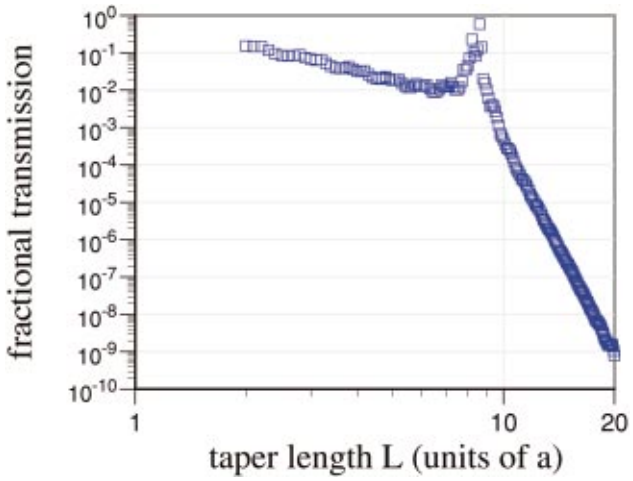

FIG. 7. (Color) Transmitted power at $\omega = 0.23 \times 2\pi c/a$ through the constant-period tapers of Fig. 4 as a function of taper length L, as computed by the ''exact'' scattering-matrix method. Transmission drops rapidly (after an initial resonance) because this frequency intersects the gap at some points in the taper (from Fig. 6).

$\partial \varepsilon_z / \partial z$ surface-integral term from the shifting boundary in the *unit-period* virtual grating.

B. Dodging the continuum

The second criterion of the adiabatic theorem is that the mode must be guided in all of the intermediate waveguides; it must never enter a continuum. This leads to a second pitfall when one wishes to couple an index-guided waveguide—such as a 1D sequence of dielectric rods in air—with a bandgap-guided waveguide—such as a line-defect waveguide in a square-lattice photonic crystal of rods with a TM band gap [1]. Two possible transitions between these structures are depicted in Fig. 9. In the index-guided waveguide, the operating mode is fundamental (there are no modes below it), but in the gap-guided waveguide the mode lies above a continuum (the lower-band modes). Somehow, one must manage to transition the mode to lie above a continuum without ever moving *through* the continuum, which would cause it to become nonguided.

One straightforward transition is to slowly ''turn on'' the crystal (increasing the rod size), as in Fig. 9(a). This, however, causes the lower-band modes to be pulled down from the light cone; inevitably, they will intersect the operating mode and it will become nonguided with poor transmission. (Here, it is clear that the mode ceases to be guided when the bulk rods are the same size as the waveguide's; the failure does not depend upon this coincidence of shapes, however.) Instead, one can simply bring the photonic crystal in from far away, as depicted in Fig. 9(b). In this case, the lower-band modes, in principle, always exist below the operating modes, but are concentrated far away; when the crystal is sufficiently far away, it can be terminated abruptly with no significant effect on the waveguided mode. Thus, adiabatic transfer is

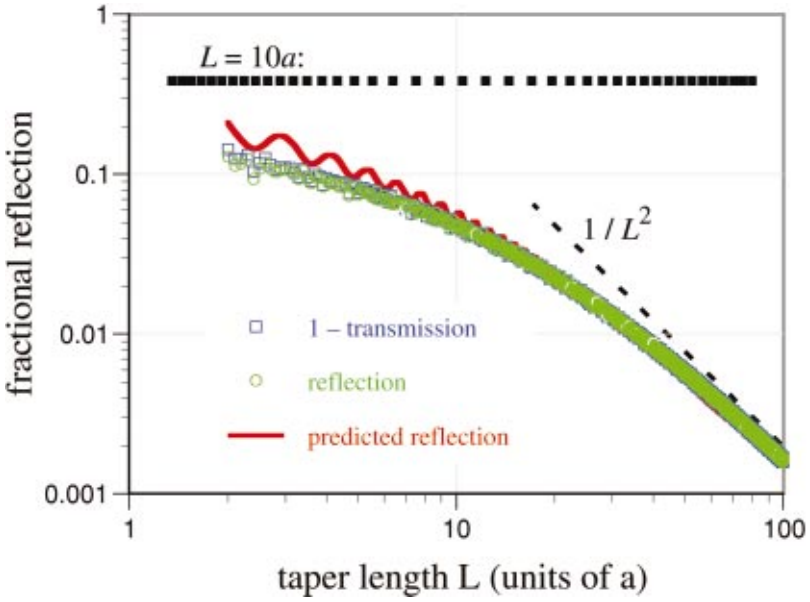

FIG. 8. (Color) Reflected power at $\omega = 0.23 \times 2\pi c/a$ from the variable-period tapers of Fig. 6 as a function of taper length L; the inset shows the $L = 10a$ structure. ''Exact'' scattering-matrix results are shown as green circles, while the solid red line is the prediction of our coupled-mode theory with the first-order approximation. Blue squares are one minus the transmission from the scattering-matrix calculation, and demonstrate that the transmission losses are dominated by reflections.

achieved. The transmission spectra for these two cases, tapering slowly into the crystal and back out again, are shown in Fig. 10 (computed by the exact scattering method) [56]. As expected, only the taper (b) that obeys the adiabatic principles demonstrates a wide bandwidth of high transmission; whereas taper (a) yields uniformly low transmission. Near the edges of the guided-mode band, even (b) exhibits Fabry-Perot oscillations due to the low group velocity in these regions—the taper would have to be longer than $10a$ to increase the transmission there. (We also computed the band diagrams of the intermediate structures for the taper design, to make sure there were not any unexpected interactions with surface states of the crystal that might cause the operating mode to become nonguided or evanescent.)

VII. CONCLUDING REMARKS

We have developed a generalization of coupled-mode theory, a set of coupled linear differential equations (25), to describe nonuniform gratings and photonic crystals in the instantaneous Bloch-mode basis. Because our formulation involves no discontinuities and centers around an explicit small parameter (the rate of change of the grating), it lends itself to effective first-order approximation (28) and other analytical study. It enables the computation of reflection and transmission for tapered gratings, and, in particular, provides an efficient method to determine how long a taper must be in order to achieve a desired level of transmission. Unlike other numerical techniques, which require more computational resolution and power as a taper becomes more gradual (and is eventually prohibitive), the coupled-mode approach becomes *more* accurate and efficient for more gradual tapers with roughly the *same* computational resources.

Moreover, we have proved that an adiabatic theorem holds even for strongly grated waveguides (photonic crystals), exactly as for nongrated waveguides, ensuring 100% transmission for sufficiently slow tapers. This theorem, however, imposes the requirements that the operating mode always be guided (discrete) and propagating (nonevanescent) for every intermediate point in the taper—requirements that are easy to inadvertently violate for transitions in photonic crystals. Fortunately, such pitfalls are simple to avoid by computing the band diagrams of all the intermediate gratings and adjusting the period or shifting the crystal accordingly. In this way, one can design efficient waveguide transitions and couplers in photonic crystals by a sequence of small eigenmode calculations on independent unit cells of the intermediate waveguides, rather than large simulations of entire tapers.

A number of future extensions are possible for this work. First, in the examples above, we showed tapers at uniform rates, whereas a more efficient transition would employ variable rates. Qualitatively, one would like to taper more slowly when $\Delta\beta$ is small and coupling is strong, and more quickly in the opposite case. Quantitatively, the optimal variable taper rate could be determined by solving a nonlinear optimization problem based on Eq. (28) (without recomputing the coupling coefficients). Moreover, one could design a taper that shifts the gap edge away as quickly as possible in order to address the difficult problem of coupling to slow-

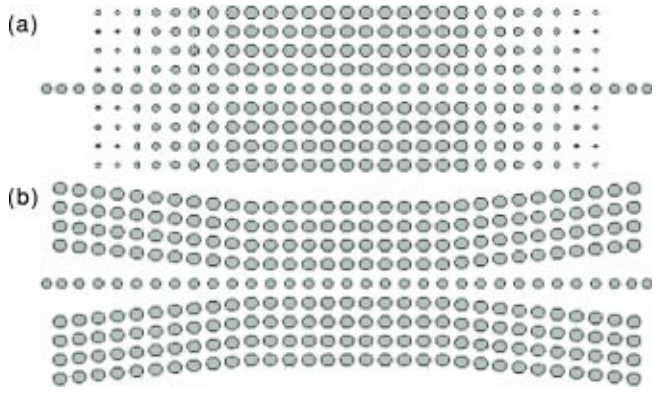

FIG. 9. Two possible tapers between a 1D sequence of dielectric rods (radius $r=0.2a$, index $n=3.37$) and an $r=0.2a$ line-defect waveguide in a square lattice of $r=0.3a$ dielectric rods in air. (a) yields low transmission because an intermediate waveguide is not guided, whereas the ''zipper'' structure (b) approaches the adiabatic limit.

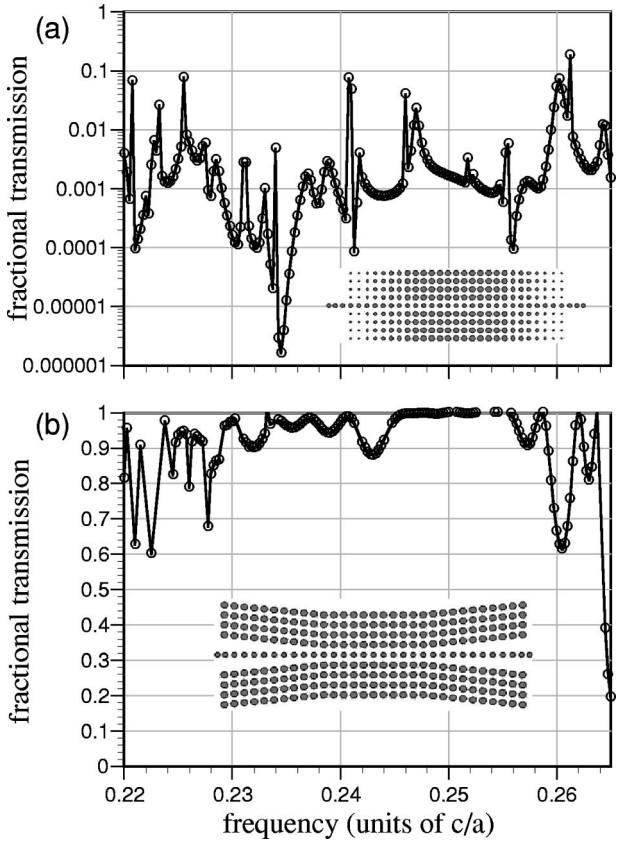

FIG. 10. Transmitted power as a function of frequency through the two taper transitions of Fig. 9 to/from a photonic-crystal line-defect waveguide. (a) exhibits the predicted low transmission (note log scale) due to intermediate points being nonguided, whereas (b) recovers the adiabatic limit of high transmission over broad bandwidth. The frequency axis ranges over the bandwidth of the guided mode (in the TM gap); i.e., the left and right edges of the graphs correspond to the band edges, where the low group velocity makes coupling difficult in a short taper.

light states near the band edge. (Much previous effort has been invested in the optimization of conventional tapers [49–52].) Numerical computations in three-dimensional systems are an application we are already addressing with another publication. Finally, our coupled-mode formulation need not be restricted to gratings in electromagnetism; it could be applied to any periodic Hermitian system (in time or space) for which the periodicity is slowly changing.

ACKNOWLEDGMENTS

This work was supported in part by the Materials Research Science and Engineering Center program of the National Science Foundation. P. B. is grateful to the Flemish Fund for Scientific Research (FWO-Vlaanderen) for support.

APPENDIX A: THE ADIABATIC THEOREM

Although the adiabatic theorem has been proven before for equivalent algebraic systems [8,38–43], we sketch a proof of it here in order to highlight its essential features, and also to point out where it fails. Suppose that we have a set of coupled linear differential equations in $c_n(z)$ describing the solution to some z-varying system,

$$\frac{dc_n}{dz} = \sum_{m \neq n} C_{mn}(z) \left\langle \frac{\partial \hat{X}}{\partial z} \right\rangle \exp\left(i \int^z \Delta\beta_{mn}(z')dz' \right) c_m(z), \tag{A1}$$

for some z-varying coefficients C_{mn}, a matrix element in terms of some operator $\hat{X}$, and phase mismatches $\Delta\beta_{mn}$. Let C_{mn}, $\hat{X}$, and $\Delta\beta_{mn}$ be independent of the rate of change of the system. (Our coupled-mode equations, as well as those from quantum mechanics, fall into this form.) We wish to understand the limit as the length L of a taper becomes long, so we introduce a scaled coordinate $s = z/L$ to separate the L dependence, in which case the equations become

$$\frac{dc_n}{ds} = \sum_{m \neq n} C_{mn}(s) \left\langle \frac{\partial \hat{X}}{\partial s} \right\rangle \exp\left(iL \int^s \Delta\beta_{mn}(s')ds' \right) c_m(s). \tag{A2}$$

The key point here is that the only L dependence appears in the exponent. It is now straightforward to take the $L \to \infty$ limit, because in that limit we have $\exp[iLf(s)] \to 0$ in the sense of generalized functions [53] for any real-valued function $f(s)$ with nonzero first derivative—it is a sinusoid that oscillates infinitely rapidly, and so integrates to zero against any smooth localized function. If the coefficients of such a differential equation over a finite domain ($s = 0 \cdots 1$) go to zero in the sense of generalized functions, then the solutions are constants $c_n(z) = c_n(0)$, which is the desired result.

It is clear from the above discussion, however, that in order to prove the adiabatic theorem here we restricted the problem in two ways: $\Delta\beta$ must be real and nonzero. Requiring that $\Delta\beta$ be nonzero is equivalent to saying that the mode must be guided—if it is not guided, it is part of a continuum of radiating modes and no finite taper length will suffice to prohibit losses. Strictly speaking, an adiabatic limit may exist even for such continua, but its approach is (in general) arbitrarily slow [40]. (Note that the $\Delta\beta = 0$ degeneracies that can arise for finitely many guided modes can typically be handled by the usual methods of degenerate perturbation theory, i.e., by choosing linear combinations that diagonalize the coupling matrix. Discrete eigenvalue crossings also do not present a problem [40].) Of course, all physical waveguides have some losses, which will prevent the fully adiabatic ideal, but this is not a concern as long as the taper length of interest is much less than the decay length of the mode. The usual adiabatic theorem also fails if the initial mode is itself exponentially decaying ($\Im[\beta] > 0$), or becomes thus at some point in the taper; in this case, all of the power is reflected in the adiabatic limit.

APPENDIX B: PHASE CONSISTENCY

In our development of the coupled-mode equations, we transformed the matrix elements $\langle m^* | \hat{B} \cdot \partial | n \rangle / \partial z$ into an equivalent expression in terms of the (known) derivative of the eigenoperator instead of the (difficult to compute) derivative of the eigenstate. (We have dropped the z subscripts for convenience.) This transformation can be understood in terms of first-order perturbation theory [32], but we instead derive it here by explicitly differentiating the eigenequation. Moreover, we show that the remaining $\langle n^* | \hat{B} \cdot \partial | n \rangle / \partial z$ self term may typically be dropped by requiring an easily satisfied phase-consistency condition.

Let us operate $\partial/\partial z$ on both sides of the eigenequation $\hat{C}_z | n \rangle = \beta_n(z) \hat{B} | n \rangle$, and then take the $\langle m^* |$ inner product with both sides. Noting that $\langle m^* | \hat{C}_z = \beta_m(z) \langle m^* | \hat{B}$ and employing the orthonormality relation (11), one obtains

$$\left\langle m^* \left| \frac{\partial \hat{C}_z}{\partial z} \right| n \right\rangle + (\beta_m - \beta_n) \langle m^* | \hat{B} \frac{\partial | n \rangle}{\partial z} = \frac{\partial \beta_n}{\partial z} \delta_{m,n} \eta_n . \tag{B1}$$

For $m \neq n$, this equation yields the desired result,

$$\langle m^* | \hat{B} \frac{\partial | n \rangle}{\partial z} = \frac{\left\langle m^* \left| \frac{\partial \hat{C}_z}{\partial z} \right| n \right\rangle}{\beta_n - \beta_m}. \tag{B2}$$

For $m = n$, on the other hand, one obtains only a trivial result. In order to eliminate this inconvenient term, however, it is often possible to choose

$$\langle n^* | \hat{B} \frac{\partial | n \rangle}{\partial z} = 0 \tag{B3}$$

merely by a proper phase-consistency convention for the instantaneous eigenstates as a function of z. In particular, consider the real-β modes that are of primary interest for adiabatic tapers; for these modes, $|n^*\rangle = |n\rangle$ and $\langle n^* | \hat{B} | n \rangle = \eta_n$ is a constant (± 1) independent of z, and thus

$$\frac{\partial}{\partial z}\langle n^*|\hat{B}|n\rangle = 0 = \left(\langle n^*|\hat{B}\,\frac{\partial|n\rangle}{\partial z}\right) + \left(\langle n^*|\hat{B}\,\frac{\partial|n\rangle}{\partial z}\right)^*, \tag{B4}$$

which implies that $\langle n^*|\hat{B}\cdot\partial|n\rangle/\partial z$ is purely imaginary. Then, one can select a new phase $|n\rangle \rightarrow e^{i\theta(z)}|n\rangle$ to fulfill the condition (B3), where θ is purely real and satisfies

$$\frac{d\theta}{dz} = i\,\eta_n^*\langle n^*|\hat{B}\,\frac{\partial|n\rangle}{\partial z}. \tag{B5}$$

(This phase θ is closely related to ''Berry's phase'' from quantum mechanics [30,31].)

There are two cases in which the phase-consistency condition is trivial to satisfy. First, in the ordinary coupled-mode theory for nongrated waveguides, assuming real ε and μ, the real-β eigenstates can be chosen to be purely real (the eigenoperators are real symmetric), in which case the phase is automatically consistent (given that the overall sign is chosen in a continuous fashion). For grated waveguides, on the other hand, the fields (Bloch modes) are not in general purely real. If the dielectric function (and μ) satisfies the common inversion symmetry $\varepsilon(-\mathbf{x}) = \varepsilon(\mathbf{x})$ (for *all* intermediate gratings), however, then the *Fourier transform* of the real-β eigenfields can be chosen as purely real [45]. In this case, because $\hat{B}$ is real-symmetric, the inner product $\langle n^*|\hat{B}\cdot\partial|n\rangle/\partial z$ is a convolution of real functions and is therefore purely real, and thus zero from Eq. (B4) above. So, again the phase requirement reduces merely to a consistent choice of sign.

When the phase-consistency requirement is not trivial, it can still be approximately satisfied numerically in a straightforward way. In the numerical implementation of coupled-mode theory, one computes the eigenstates $|n\rangle_z$ at a discrete set of z values separated by some Δz, and need therefore to choose the phase of $|n\rangle_{z+\Delta z}$ relative to that of $|n\rangle_z$. Using these states to compute the finite-difference approximation to Eq. (B3), this equation can then be best satisfied by $e^{i\theta}|n\rangle_{z+\Delta z}$, where $\theta = -\arg[\,\eta_n^*\langle n^*|_z\hat{B}|n\rangle_{z+\Delta z}]$.

[1] J. D. Joannopoulos, R. D. Meade, and J. N. Winn, *Photonic Crystals: Molding the Flow of Light* (Princeton University Press, Princeton, NJ, 1995).

[2] A. Mekis, J. C. Chen, I. Kurland, S. Fan, P. R. Villeneuve, and J. D. Joannopoulos, Phys. Rev. Lett. **77**, 3787 (1996).

[3] S. Fan, S. G. Johnson, J. D. Joannopoulos, C. Manolatou, and H. A. Haus, J. Opt. Soc. Am. B **18**, 162 (2001).

[4] S. Fan, P. R. Villeneuve, J. D. Joannopoulos, and H. A. Haus, Phys. Rev. Lett. **80**, 960 (1998).

[5] M. Soljačić, M. Ibanescu, S. G. Johnson, Y. Fink, and J. D. Joannopoulos, Phys. Rev. E **66**, 055601(R) (2002).

[6] M. Soljačić, S. G. Johnson, S. Fan, M. Ibanescu, E. Ippen, and J. D. Joannopoulos, J. Opt. Soc. Am. B **19**, 2052 (2002).

[7] A. Yariv, Y. Xu, R. K. Lee, and A. Scherer, Opt. Lett. **24**, 711 (1999).

[8] D. Marcuse, *Theory of Dielectric Optical Waveguides*, 2nd ed. (Academic Press, San Diego, 1991).

[9] Y. Xu, R. K. Lee, and A. Yariv, Opt. Lett. **25**, 755 (2000).

[10] A. Mekis and J. D. Joannopoulos, J. Lightwave Technol. **19**, 861 (2001).

[11] M. Palamaru and P. Lalanne, Appl. Phys. Lett. **78**, 1466 (2001).

[12] T. D. Happ, M. Kamp, and A. Forchel, Opt. Lett. **26**, 1102 (2001).

[13] P. Rabiei and A. F. J. Levi, CLEO postdeadline papers (2001), pp. 590–591.

[14] P. Sanchis, J. Marti, A. Garcia, A. Martinez, and J. Blasco, Electron. Lett. **38**, 961 (2002).

[15] B. Z. Katsenelenbaum, L. Mercader del Río, M. Pereyaslavets, M. Sorolla Ayza, and M. Thumm, *Theory of Nonuniform Waveguides: The Cross-Section Method* (Inst. of Electrical Engineers, London, 1998).

[16] K. S. Kunz and R. J. Luebbers, *The Finite-Difference Time-Domain Method for Electromagnetics* (CRC Press, Boca Raton, 1993).

[17] P. M. Bell, J. B. Pendry, L. M. Moreno, and A. J. Ward, Comput. Phys. Commun. **85**, 306 (1995).

[18] J. Willems, J. Haes, and R. Baets, Opt. Quantum Electron. **27**, 995 (1995).

[19] E. Silberstein, P. Lalanne, and J.-P. Hugonin, J. Opt. Soc. Am. A **18**, 2865 (2001).

[20] G.-W. Chern, L. A. Wang, and C.-Y. Lin, Appl. Opt. **40**, 4476 (2001).

[21] P. Bienstman and R. Baets, Opt. Quantum Electron. **33**, 327 (2001).

[22] W.-P. Huang, J. Opt. Soc. Am. A **11**, 963 (1994).

[23] A. Yariv, *Optical Electronics in Modern Communication*, 5th ed. (Oxford University Press, Oxford, 1997).

[24] H. A. Haus, *Waves and Fields in Optoelectronics* (Prentice-Hall, Englewood Cliffs, NJ, 1984).

[25] B. M. A. Rahman, N. Mahmood, J. M. Gomoluch, N. Anwar, and K. T. V. Grattan, Proc. SPIE **4532**, 261 (2001).

[26] N. Matuschek, F. X. Kärtner, and U. Keller, IEEE J. Quantum Electron. **33**, 295 (1997).

[27] R. H. Young and W. J. Deal, Jr., J. Math. Phys. **11**, 3298 (1970).

[28] D. W. Hone, R. Ketzmerick, and W. Kohn, Phys. Rev. A **56**, 4045 (1997).

[29] T. Iizuka and C. M. de Sterke, Phys. Rev. E **61**, 4491 (2000).

[30] J. J. Sakurai, *Modern Quantum Mechanics*, revised edition (Addison-Wesley, Reading, MA, 1994).

[31] M. V. Berry, Proc. R. Soc. London, Ser. A **392**, 45 (1984).

[32] C. Cohen-Tannoudji, B. Din, and F. Laloë, *Quantum Mechanics* (Hermann, Paris, 1977), Vol. 1, Chap. 2; and Vol. 2, Chaps. 11 and 13.

[33] P. A. M. Dirac, *Principles of Quantum Mechanics* (Clarendon, Oxford, 1982).

[34] S. G. Johnson, M. Ibanescu, M. Skorobogatiy, O. Weisberg, T. D. Engeness, M. Soljačić, S. A. Jacobs, J. D. Joannopoulos, and Y. Fink, Opt. Express **9**, 748 (2001), URL:http://www.opticsexpress.org/abstract.cfm?URI=OPEX-9-13-748

[35] M. Skorobogatiy, M. Ibanescu, S. G. Johnson, O. Weisberg, T. D. Engeness, M. Soljačić, S. A. Jacobs, and Y. Fink, J. Opt. Soc. Am. B (to be published).
[36] S. G. Johnson, M. Ibanescu, M. A. Skorobogatiy, O. Weisberg, J. D. Joannopoulos, and Y. Fink, Phys. Rev. E **65**, 066611 (2002).
[37] N. W. Ashcroft and N. D. Mermin, *Solid State Physics* (Holt Saunders, Philadelphia, 1976).
[38] A. Messiah, *Quantum Mechanics: Vol. II* (Wiley, New York, 1976), Chap. 17.
[39] G. Nenciu, J. Phys. A **13**, L15 (1980).
[40] J. E. Avron and A. Elgart, Commun. Math. Phys. **203**, 445 (1999).
[41] R. H. Young and W. J. A. Deal, Jr., Phys. Rev. A **1**, 419 (1970).
[42] A. G. Chirkov, Tech. Phys. Lett. **27**, 14 (2001).
[43] T. Kato, Phys. Soc. Jpn. **5**, 435 (1950).
[44] P. R. Villeneuve, S. Fan, S. G. Johnson, and J. D. Joannopoulos, IEE Proc.: Optoelectron. **145**, 384 (1998).
[45] S. G. Johnson and J. D. Joannopoulos, Opt. Express **8**, 173 (2001); URL:http://www.opticsexpress.org/abstract.cfm?URI=OPEX-8-3-173
[46] W. H. Press, S. A. Teukolsky, W. T. Vetterling, and B. P. Flannery, *Numerical Recipes in C: The Art of Scientific Computing*, 2nd ed. (Cambridge University Press, Cambridge, 1992).
[47] J. P. Bérenger, J. Comput. Phys. **114**, 185 (1994).
[48] P. Bienstman, software at http://camfr.sf.net
[49] W. K. Burns, A. F. Milton, and A. B. Lee, Appl. Phys. Lett. **30**, 28 (1977).
[50] V. K. Kiseliov, Int. J. Infrared Millim. Waves **21**, 163 (2000).
[51] C.-T. Lee, M.-L. Wu, L.-G. Sheu, P.-L. Fand, and J.-M. Hsu, J. Lightwave Technol. **15**, 403 (1997).
[52] T. A. Ramadan, R. Scarmozzino, and R. M. Osgood, Jr., J. Lightwave Technol. **16**, 277 (1998).
[53] I. M. Gel'fand and G. E. Shilov, *Generalized Functions* (Academic Press, New York, 1964).
[54] One of the terms in Eq. (6) can be eliminated by adding $\langle\beta^*|\hat{B}|\beta'\rangle+\langle\beta^*|\hat{B}|-\beta'\rangle$ and exploiting time-reversal invariance.
[55] We are always free to choose that $c_{m,k}(0)$ be concentrated in $k=0$, since the k index is artificial.
[56] In addition to the taper to/from the photonic crystal, the rod sequence is tapered adiabatically to/from a uniform waveguide at the edges of the computational cell to eliminate reflections, using the method of Sec. VI A A (reducing the period until the rods merge).